

Different Spectral Signatures of Octapeptide 3_{10} - and α -Helices Revealed by Two-Dimensional Infrared Spectroscopy

Hiroaki Maekawa,[†] Claudio Toniolo,[‡] Alessandro Moretto,[‡] Quirinus B. Broxterman,[§] and Nien-Hui Ge^{*,†}

Department of Chemistry, University of California, Irvine, California, 92697-2025, Department of Chemistry, University of Padova, 35131 Padova, Italy, and DSM Research, Life Sciences, Advanced Synthesis and Catalysis, P.O. Box 18, 6160 MD Geleen, The Netherlands

Received: December 22, 2005; In Final Form: January 31, 2006

Femtosecond two-dimensional infrared (2D IR) spectroscopy is applied to the amide I modes of the terminally protected homo-octapeptide Z-[L-(α Me)Val]₈-OtBu in CDCl₃, 2,2,2-trifluoroethanol (TFE), and 1,1,1,3,3,3-hexafluoro-2-propanol (HFIP) solutions to acquire 2D spectral signatures that distinguish between 3_{10} - and α -helix structures. Suppression of diagonal peaks by controlling polarizations of IR pulses clearly reveals cross-peak patterns that are crucial for structural determination. A doublet feature is observed when the peptide ester forms a 3_{10} -helix in CDCl₃ and TFE and when it is at the initial stage of 3_{10} - to α -helix transition in HFIP. In contrast, the 2D IR spectrum shows a multiple peak pattern after the peptide ester has acidolyzed and become an α -helix in HFIP. Electronic circular dichroism spectra accompanying the acidolysis-driven conformational change are also reported. This is the first report on the experimental 2D IR signature of a 3_{10} -helical peptide. These results, using a model octapeptide, demonstrate the powerful capability of 2D IR spectroscopy to discriminate between different helical structures.

The 3_{10} -helix constitutes a small but significant percentage of secondary structural elements in proteins.^{1,2} According to a general survey of protein structures, about 10% of all helices adopt the 3_{10} -helical conformation in which an intramolecular hydrogen bond is formed between the C=O group of the i th amino acid residue and the N-H group of the ($i + 3$) residue ($i + 4$ for the α -helix).³ The 3_{10} -helices are mainly observed at the termini of α -helices, in loops, and as connectors between β -strands, with an average length of 3.3 residues. They play important functional roles in several proteins.^{4–6} Some trans-membrane channel-forming antibiotics, such as alamethicin, have a high content of 3_{10} -helices.⁷ Moreover, the 3_{10} -helix structure has recently been proposed as an intermediate in the folding of α -helices^{2,8} and is observed as picosecond intermediates in simulation studies of α -helix melting.^{9,10} To fully understand helix formation processes, including nucleation and formation of nascent helices, theoretical findings should be combined with experimental techniques that have not only a high sensitivity to subtle structural differences between 3_{10} - and α -helices but also a picosecond time resolution.

Several spectroscopic techniques are useful for solving structures of biological molecules in solids, solutions, and membranes.¹¹ In fact, electronic and vibrational circular dichroism (ECD and VCD) and 2D NMR measurements have successfully identified 3_{10} -helical structures of synthetic model oligopeptides in nonaqueous solution phases.^{12–15} Because of

insufficient time resolution, however, these techniques cannot discriminate between the two helices during the earliest steps of helix formation processes. Although time-resolved linear-IR spectroscopy can be performed on femtosecond and picosecond time scales, a diagnostic peak frequency of the amide I band is often ambiguous, especially for short 3_{10} - and α -helix structures.^{16,17} The IR peak frequency is influenced by several factors, including helical length, types of amino acid residues, structural deformation, and solvent exposure. A recent ab initio density functional theory study also shows that the amide I maximum in linear-IR spectra cannot be used to discriminate between 3_{10} - and α -helices.¹⁸

We believe that two-dimensional infrared (2D IR) spectroscopy^{19–35} is the most promising technique for studying 3_{10} - to α -helix transition, because it can be used to obtain a cross-peak pattern of the amide I modes.^{20–31} Cross-peaks appear in 2D IR spectra only if the vibrational modes are coupled, and the coupling strength acutely depends on the underlying structure. For peptides and proteins, the through-space couplings between the nonadjacent amide I vibrators can be approximated by the transition dipole–dipole interaction that depends on the angles and distances between the dipoles.³⁶ The through-bond couplings between nearest-neighboring amide groups depend on dihedral angles of the peptide backbone and have been mapped out by ab initio calculations.³⁷ The 3_{10} - and α -helical structures are different in their dihedral angles [$(\phi, \psi) = (-57^\circ, -30^\circ)$ and $(-63^\circ, -42^\circ)$ for right-handed 3_{10} - and α -helix, respectively],¹ pitch, rotation per residue, and hydrogen bond geometry, and hence, their 2D IR spectral pattern is expected to be different. Theoretical studies on long (> 15 residues) 3_{10} -

* To whom correspondence should be addressed. Email address: nhge@uci.edu. Phone: 949-824-1263. Fax: 949-824-8571.

[†] University of California.

[‡] University of Padova.

[§] DSM Research.

and α -helical model peptides have also been performed to examine the helical structure sensitivity of 2D IR spectroscopy.^{30,31} Furthermore, the time resolution of 2D IR spectroscopy is less than a few picoseconds for the amide I bands of small peptides and proteins as determined by the time required to fully characterize the decay of vibrational coherences created and manipulated by femtosecond IR pulses.^{20–29} These unique characteristics of 2D IR spectroscopy have made it a powerful tool to elucidate structure and dynamics of peptides and proteins.^{20–31}

In this paper, the 2D IR spectroscopy is applied to the amide I modes of the terminally protected homo-octapeptide Z-[L-(α Me)Val]₈-OrBu (Z, benzyloxycarbonyl; (α Me)Val, C $^{\alpha}$ -methyl valine; OrBu, *tert*-butoxy) in several organic solvents to experimentally acquire characteristic spectral signatures for 3_{10} - and α -helical structures. The average backbone dihedral angles of Z-[L-(α Me)Val]₈-OrBu in the crystal state^{12,38} are very close to those of short 3_{10} -helices in proteins.^{1,3} Previous ECD, VCD, and 2D NMR measurements concluded that the strictly related N $^{\alpha}$ -acetylated homo-octapeptide, Ac-[L-(α Me)Val]₈-OrBu (Ac, acetyl), forms a stable 3_{10} -helix in CDCl₃ solution and an α -helix in some fluoro alcohols after a slow 3_{10} - to α -helix transition on a time scale of days.^{13,14} This interesting feature suggests that one could make a direct comparison of 2D IR spectra between the two helix types of the Z-protected peptide in the same solvent. We show that the 2D IR cross-peak pattern of the amide I modes clearly reflects the differences in these helical structures.

Details of our experimental setup and measurements of 2D IR spectra are described in the Supporting Information. In brief, three 100-fs IR pulses with a 1660 cm⁻¹ central frequency and wavevectors of k_a , k_b , and k_c were focused on a sample solution to induce the third-order resonant signal of the amide I modes. The signal was heterodyne-detected at the phase-matching direction of $-\mathbf{k}_a + \mathbf{k}_b + \mathbf{k}_c$ by a local oscillator pulse with a wavevector \mathbf{k}_{LO} . The experiments were conducted using a pulse sequence of a–b–c, where the time delays were τ between k_a and k_b , T between k_b and k_c , and t between k_c and k_{LO} pulses. Absolute magnitude of 2D IR spectra $S(-\omega_\tau, \omega_t)$ were obtained by 2D Fourier transform of the data matrix along τ and t at fixed $T = 0$. Measurements were mainly taken under the polarization configuration of $\langle \pi/4, -\pi/4, Y, Z \rangle$ to suppress diagonal peaks and to clearly reveal cross-peaks between the amide I modes (see the Supporting Information).^{22,32} In these measurements, the typical cross-peak intensity is larger than the residual diagonal peak intensity by at least 1 order of magnitude.

Z-[L-(α Me)Val]₈-OrBu was synthesized and characterized as described in previous work.^{12,38} The octapeptide ester was dissolved in CDCl₃ (Cambridge Isotope Laboratories, 99.96% D) to generate a stable 3_{10} -helical structure. To induce an α -helical conformation, the peptide was dissolved in 1,1,1,3,3,3-hexafluoro-2-propanol (HFIP) (Acros Organics, 99.5%) in parallel experiments. Another fluoro alcohol, 2,2,2-trifluoroethanol (TFE) (Acros Organics, 99.8%), was also used as a comparison. These solvents were used without further purification. Peptide concentration in each solution was about 10 mM so that the optical density of the amide I band was about 0.3 in a 100- μ m-thick CaF₂ sample cell.

In CDCl₃ and in TFE, the amide I band of Z-[L-(α Me)Val]₈-OrBu is observed at 1659 and 1658 cm⁻¹, respectively, as shown in the FT IR spectra (Figure 1a). The C-protecting *tert*-butyl ester and N-protecting urethane C=O bands are located at 1715–1720 cm⁻¹ and are not resolved in these solvents.¹³

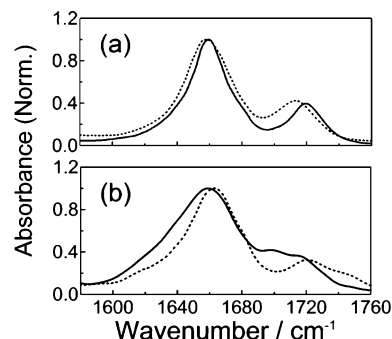


Figure 1. Solvent- and time-dependent FT IR spectra of Z-[L-(α Me)-Val]₈-OrBu: (a) in CDCl₃ (solid line), TFE (dashed line); (b) in HFIP measured immediately (solid line), and 34 days (dashed line) after sample preparation. The background spectrum of the neat solvent is subtracted, and each spectrum is normalized by the peak absorbance of the amide I band at around 1660 cm⁻¹.

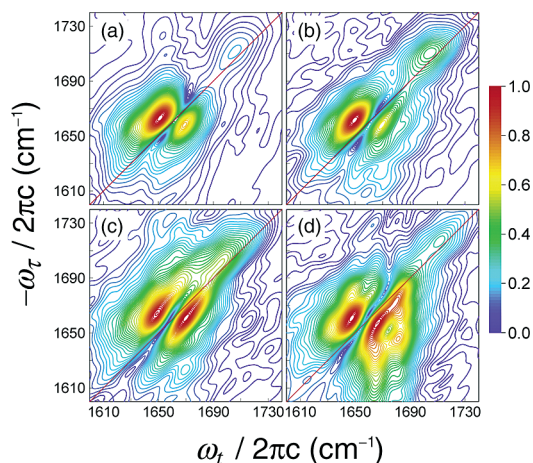


Figure 2. 2D IR absolute magnitude spectra of Z-[L-(α Me)Val]₈-OrBu measured under $\langle \pi/4, -\pi/4, Y, Z \rangle$ polarization configuration in different solvents: (a) CDCl₃; (b) TFE; (c,d) HFIP. The spectra in HFIP were measured (c) immediately and (d) 34 days after sample preparation. All spectra are normalized by the peak maximum and plotted with 40 equally spaced contour lines between 0 and 1.

Although the peptide exhibits a single, featureless amide I band in its FT IR spectra, a distinct cross-peak pattern appears in its 2D IR spectra. The absolute magnitude of the 2D IR spectrum measured in CDCl₃ with a polarization configuration of $\langle \pi/4, -\pi/4, Y, Z \rangle$ (Figure 2a) exhibits a clear doublet feature at $(-\omega_\tau, \omega_t) = (1663, 1651)$ and $(1658, 1669)$ cm⁻¹. A very similar spectrum with a clear doublet feature is also obtained for this peptide in TFE (Figure 2b) and for two Aib (α -aminoisobutyric acid)-rich octapeptides, Z-(Aib)₈-OrBu and Z-(Aib)₅-L-Leu-(Aib)₂-OMe, in CDCl₃ at 5 mM concentration (data not shown). These Aib-based peptides adopt a stable, concentration-independent 3_{10} -helical conformation in CDCl₃.^{39,40} The results suggest that this doublet in the amide I frequency region may be considered a general 2D IR signature of short 3_{10} -helical peptides, regardless of the length of the alkyl side chains, the solvents, the terminally protecting groups, and the effects from interpeptide interactions. This unique cross-peak pattern results from couplings between all amide I modes along the peptide backbone and cannot be assigned to transitions on specific residues. The entire vibrational excitonic band may not only include the strong doublet feature but also the weak peak located at the higher transition frequency region near (1711, 1706) cm⁻¹.

In HFIP, significant changes in the FT IR spectra are observed as a function of time (Figure 1b). Immediately after dissolving Z-[L-(α Me)Val]₈-OrBu, the amide I band peaks at 1659 cm⁻¹.

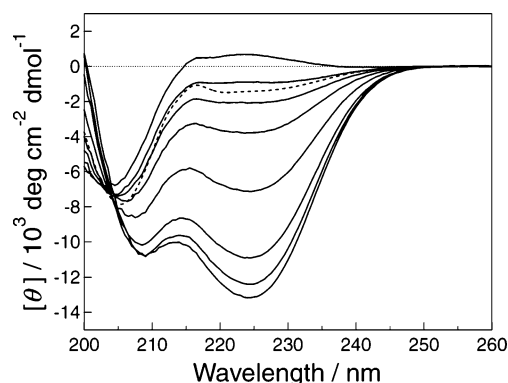


Figure 3. Time-dependent ECD spectra of Z-[L-(α Me)Val]₈-OrBu in HFIP solution (solid lines). From top to bottom at 222 nm, the spectrum was measured immediately and 2, 4, 7, 13, 18, 21, and 34 days after sample preparation. A spectrum measured in TFE, 19 days after preparation, is also shown for comparison (dashed line). Molar ellipticity $[\theta]$ is normalized by the number of L-(α Me)Val residues.

The urethane and ester C=O bands are partially resolved and located at 1700 and 1715 cm^{-1} , respectively.⁴¹ At 34 days, the amide I peak becomes blue-shifted by 4 cm^{-1} , and its line width narrows. Drastic changes are also seen for the terminal C=O bands. We attribute these spectral changes to the slow conversion of the octapeptide *tert*-butyl ester into its free acid derivative which, in turn, undergoes rapid 3₁₀- to α -helix transition.⁴² Acidolysis results in the disappearance of the ester C=O peak and the appearance of the carboxylic acid C=O stretching mode at around 1745 cm^{-1} . Conformational transition results in changes in the amide I band and the urethane C=O, as they are known to be sensitive to secondary structure and local environment.⁴¹ No further changes of the FT IR spectrum were observed beyond 34 days, indicating the completion of acidolysis and conformational transitions.

The helical transition of Z-[L-(α Me)Val]₈-OrBu in HFIP solution was further monitored with ECD measurements (Figure 3). The most significant time-dependent change is the intensity ratio between two negative peaks at 208 and 222 nm ($R = \{[\theta]_{222}/[\theta]_{208}\}$). It was theoretically and experimentally suggested that R would be indicative of different helical structures: $R \ll 1$ for the 3₁₀-helix and $R \approx 1$, or as large as 1.4, for the α -helix.^{43,44} This diagnostic feature in ECD spectra was experimentally verified for two related peptides that underwent 3₁₀- to α -helix transition.^{12–15} Even though the aromatic ring of the Z-protected group might slightly affect our ECD spectra in the far-UV region, the increase of R over time is similar to that observed for the Ac-blocked peptide in HFIP,^{13,14} indicating that the 3₁₀- to α -helix transition also occurs in the Z-protected peptide.

Although the initial ECD spectrum does not fully match that of a typical 3₁₀-helix, it cannot be attributed to either a statistical coil or a semi-extended, rigid, polyproline II (P_{II})-like structure. The negative Cotton effect of these conformations is usually seen at ~ 190 – 198 nm,^{43,45} not at 204 nm as in our case. The positive Cotton effect of the P_{II} conformation is a clear band centered at ~ 215 nm, not a broad, featureless dichroic absorption as in our spectrum. Moreover, C α -methylated α -amino-acid residues extremely rarely adopt the P_{II} conformation, because the conformational energy for these residues is too high in the $(\phi, \psi) = (-70^\circ, 145^\circ)$ region.⁴⁶ The unusual initial ECD spectrum suggests that the 3₁₀-helix is partially distorted from its regular ϕ and ψ angles due to strong solvation by HFIP. The distortion effect is also manifested in the initial broadening of the amide I band, as well as in the frequency shift of the

urethane C=O stretch (Figure 1b, solid line), as compared to those observed in TFE and CDCl₃ (Figure 1a).

To further investigate the solvent effect, the ECD spectrum was recorded in TFE immediately (data not shown) and 19 days after sample preparation (Figure 3, dashed line). TFE is a weaker hydrogen-bond donor compared to HFIP; therefore, less marked solvation and distortion of the peptide backbone are expected. Not surprisingly, the initial spectrum does not exhibit the positive Cotton effect. Also, the spectrum does not change much within 19 days, indicating that the acidolysis and subsequent transition from 3₁₀- to α -helix proceed at a much slower rate than when in HFIP. TFE is much less acidic than HFIP and, therefore, is much less capable of cleaving the *tert*-butyl ester bond.

Following confirmation that the Z-protected peptide undergoes the 3₁₀- to α -helix transition in HFIP using conventional techniques, we then applied 2D IR to see if this technique would exhibit different spectral signatures for the two conformations. Parts c and d of Figure 2 present the 2D IR spectra measured in HFIP immediately and 34 days after sample preparation, respectively. At the initial stage, a doublet feature emerges. It is similar to that observed in CDCl₃ and TFE except that the spectral shape is more elongated along the diagonal line and the intensity ratio of the doublet is different (Figure 2c). While the doublet characteristic of a 3₁₀-helix is maintained in the initial exposure to HFIP, the elongation of the peaks indicates the presence of a large inhomogeneous distribution of amide I mode frequencies. In contrast, the 2D spectrum measured after 34 days (Figure 2d) exhibits a different pattern as the acidolysis and conformational transition reaches completion. Several additional peaks clearly appear around the intense doublet feature, which are not observed for the peptide ester with a stable 3₁₀-helix form in CDCl₃ or TFE or at the initial measurement in HFIP.

The time evolution of the 2D IR cross-peak pattern of the L-(α Me)Val homo-octapeptide in HFIP highlights the change in the amide I mode vibrational couplings that accompanies the 3₁₀- to α -helix conformational transition. Although Figure 2c corresponds to Z-[L-(α Me)Val]₈-OrBu and Figure 2d to Z-[L-(α Me)Val]₈-OH, we do not expect the difference in the C-termini to qualitatively affect the cross-peak patterns, because the carboxylic acid and ester C=O stretches are quite separated from the amide I modes in frequencies. Previous 2D NMR and molecular dynamics simulations of the strictly related Ac-blocked octapeptide show that, after it completes the 3₁₀ \rightarrow α transition in HFIP and is redissolved in TFE, it forms an α -helix with two 3₁₀-like hydrogen bonds at the N-terminus.¹⁴ If the Z-blocked peptide also adopts this kind of 3₁₀/ α mixed conformation (with a largely predominant α -helix contribution) in HFIP, the 2D IR spectral pattern in Figure 2d would reflect the concomitant occurrence of two helices in the same peptide. However, even though the doublet cross-peak resembles that observed for the peptide forming 3₁₀-helix over the entire range of L-(α Me)Val residues, it does not necessarily mean that the residues forming the 3₁₀-helix at the N-terminus generate this doublet and those forming the α -helix produce the additional cross-peaks. The amide I modes at the 3₁₀- and α -helical regions are still coupled to one another by through-space and through-bond interactions. Therefore, it is reasonable to consider that all vibrational couplings over the entire peptide are weaved into the observed cross-peak pattern. Analysis of the NMR structures of the Ac-blocked peptide suggests that the 3₁₀- to α - transition can result in dramatic changes in the nearest-neighbor through-bond couplings along the backbone, ranging from 0.3 to 4 times

difference. The through-space couplings are also affected by the conformational transition. The strongest nonnearest transition dipole coupling is found between the amide I modes in the i and $i + 2$ residues for the 3_{10} -helix, but between i and $i + 3$ residues for the α -helix. Such changes in vibrational couplings are expected to be reflected in the 2D IR spectral patterns. In addition, the intramolecular hydrogen bond between the acetyl C=O group and the N—H group of the third L-(α Me)Val residue is, on the average, 19% shorter and more linear in the $3_{10}/\alpha$ helix structure than in the 3_{10} -helix structure.¹⁴ This type of local structural change may also occur around the urethane C=O group of the Z-blocked peptide and manifest as the frequency change observed in FT IR spectra. Simulations of 2D spectra based on the third-order nonlinear response theory and a vibrational exciton model are currently being performed on model octapeptides in 3_{10} - and α -helix conformations. Further theoretical studies, including molecular dynamics simulations and quantum chemical calculations, are underway in order to achieve quantitative agreement with our experiments. The present results demonstrate that 2D IR spectroscopy can provide diagnostic cross-peak patterns for distinguishing different helical structures. Further development of this powerful structural tool will open avenues for elucidating the role of the 3_{10} -helix in early protein folding events.

Acknowledgment. We thank Z. Guan, S. C. Tsai, and J. S. Nowick for valuable discussions. This research was supported by the American Chemical Society Petroleum Research Fund (39148-G6) and the National Science Foundation CAREER Award (CHE-0450045) to N.-H.G.

Supporting Information Available: Detailed explanations of the 2D IR, FT IR, and ECD spectral measurements. This material is available free of charge via the Internet at <http://pubs.acs.org>.

References and Notes

- (1) Toniolo, C.; Benedetti, E. *Trends Biochem. Sci.* **1991**, *16*, 350.
- (2) Bolin, K. A.; Millhauser, G. L. *Acc. Chem. Res.* **1999**, *32*, 1027.
- (3) Barlow, D. J.; Thornton, J. M. *J. Mol. Biol.* **1988**, *201*, 601.
- (4) De Guzman, R. N.; Wu, Z. R.; Stalling, C. C.; Pappalardo, L.; Borer, P. N.; Summers, M. F. *Science* **1998**, *279*, 384.
- (5) Hashimoto, Y.; Kohri, K.; Kaneko, Y.; Morisaki, H.; Kato, T.; Ikeda, K.; Nakanishi, M. *J. Biol. Chem.* **1998**, *273*, 16544.
- (6) Matsushima, N.; Enkhbayar, P.; Kamiya, M.; Osaki, M.; Kretsinger, R. H. *Drug Des. Rev.* **2005**, *2*, 305.
- (7) Nagaraj, R.; Balaram, P. *Acc. Chem. Res.* **1981**, *14*, 356.
- (8) Shea, J. E.; Brooks, C. L. *Annu. Rev. Phys. Chem.* **2001**, *52*, 499.
- (9) Tirado-Rives, J.; Jorgensen, W. L. *Biochemistry* **1991**, *30*, 3864.
- (10) Soman, K. V.; Karimi, A.; Case, D. A. *Biopolymers* **1991**, *31*, 1351.
- (11) Sauer, K. *Methods Enzymol.* **1995**, *246*, 1.
- (12) Toniolo, C.; Polese, A.; Formaggio, F.; Crisma, M.; Kamphuis, J. *J. Am. Chem. Soc.* **1996**, *118*, 2744.
- (13) Yoder, G.; Polese, A.; Silva, R. A. G. D.; Formaggio, F.; Crisma, M.; Broxterman, Q. B.; Kamphuis, J.; Toniolo, C.; Keiderling, T. A. *J. Am. Chem. Soc.* **1997**, *119*, 10278.
- (14) Mammi, S.; Rainaldi, M.; Bellanda, M.; Schievano, E.; Peggion, E.; Broxterman, Q. B.; Formaggio, F.; Crisma, M.; Toniolo, C. *J. Am. Chem. Soc.* **2000**, *122*, 11735.
- (15) Pengo, P.; Pasquato, L.; Moro, S.; Brigo, A.; Fogolari, F.; Broxterman, Q. B.; Kaptein, B.; Scrimin, P. *Angew. Chem., Int. Ed.* **2003**, *42*, 3388.
- (16) Martinez, G.; Millhauser, G. J. *Struct. Biol.* **1995**, *114*, 23.
- (17) Silva, R. A. G. D.; Yasui, S. C.; Kubelka, J.; Formaggio, F.; Crisma, M.; Toniolo, C.; Keiderling, T. A. *Biopolymers* **2002**, *65*, 229.
- (18) Kubelka, J.; Silva, R. A. G. D.; Keiderling, T. A. *J. Am. Chem. Soc.* **2002**, *124*, 5325.
- (19) Mukamel, S. *Annu. Rev. Phys. Chem.* **2000**, *51*, 691.
- (20) Hamm, P.; Lim, M.; Hochstrasser, R. M. *J. Phys. Chem. B* **1998**, *102*, 6123.
- (21) Asplund, M. C.; Zanni, M. T.; Hochstrasser, R. M. *Proc. Natl. Acad. Sci. U.S.A.* **2000**, *97*, 8219.
- (22) Zanni, M. T.; Ge, N.-H.; Kim, Y. S.; Hochstrasser, R. M. *Proc. Natl. Acad. Sci. U.S.A.* **2001**, *98*, 11265.
- (23) Woutersen, S.; Pfister, R.; Hamm, P.; Mu, Y.; Kosov, D. S.; Stock, G. *J. Chem. Phys.* **2002**, *117*, 6833.
- (24) Fang, C.; Wang, J.; Kim, Y. S.; Charnley, A. K.; Barber-Armstrong, W.; Smith, A. B., III; Decatur, S. M.; Hochstrasser, R. M. *J. Phys. Chem. B* **2004**, *108*, 10415.
- (25) Rubtsov, I. V.; Wang, J.; Hochstrasser, R. M. *Proc. Natl. Acad. Sci. U.S.A.* **2003**, *100*, 5601.
- (26) Mukherjee, P.; Krummel, A. T.; Fulmer, E. C.; Kass, I.; Arkin, I. T.; Zanni, M. T. *J. Chem. Phys.* **2004**, *120*, 10215.
- (27) Demirdöven, N.; Cheatum, C. M.; Chung, H. S.; Khalil, M.; Knoester, J.; Tokmakoff, A. *J. Am. Chem. Soc.* **2004**, *126*, 7981.
- (28) Chung, H. S.; Khalil, M.; Tokmakoff, A. *J. Phys. Chem. B* **2004**, *108*, 15332.
- (29) Bredenbeck, J.; Helbing, J.; Behrendt, R.; Renner, C.; Moroder, L.; Wachtveitl, J.; Hamm, P. *J. Phys. Chem. B* **2004**, *107*, 8654.
- (30) Moran, A. M.; Park, S.-M.; Dreyer, J.; Mukamel, S. *J. Chem. Phys.* **2003**, *118*, 3651.
- (31) Wang, J.; Hochstrasser, R. M. *Chem. Phys.* **2004**, *297*, 195.
- (32) Hochstrasser, R. M. *Chem. Phys.* **2001**, *266*, 273.
- (33) Khalil, M.; Demirdöven, N.; Tokmakoff, A. *J. Phys. Chem. A* **2003**, *107*, 5258.
- (34) Asbury, J. B.; Steinel, T.; Kwak, K.; Corcelli, S. A.; Lawrence, C. P.; Skinner, J. L.; Fayer, M. D. *J. Chem. Phys.* **2004**, *121*, 12431.
- (35) Cowan, M. L.; Bruner, B. D.; Huse, N.; Dwyer, J. R.; Chugh, B.; Nibbering, E. T. J.; Elsaesser, T.; Miller, R. J. D. *Nature (London)* **2005**, *434*, 199.
- (36) Krimm, S.; Bandekar, J. *Adv. Protein Chem.* **1986**, *38*, 181.
- (37) Torii, H.; Tasumi, M. *J. Raman Spectrosc.* **1998**, *29*, 81.
- (38) Polese, A.; Formaggio, F.; Crisma, M.; Valle, G.; Toniolo, C.; Bonora, G. M.; Broxterman, Q. B.; Kamphuis, J. *Chem.—Eur. J.* **1996**, *2*, 1104.
- (39) Kennedy, D. F.; Crisma, M.; Toniolo, C.; Chapman, D. *Biochemistry* **1991**, *30*, 6541.
- (40) Yasui, S. C.; Keiderling, T. A.; Formaggio, F.; Bonora, G. M.; Toniolo, C. *J. Am. Chem. Soc.* **1986**, *108*, 4988.
- (41) Plass, M.; Griehl, C.; Kolbe, A. J. *Mol. Struct.* **2001**, *570*, 203.
- (42) Toniolo, C.; Moretto, A.; Formaggio, F.; Crisma, M.; Broxterman, Q. B.; Keiderling, T. A. Manuscript in preparation.
- (43) Manning, M. C.; Woody, R. W. *Biopolymers* **1991**, *31*, 569.
- (44) Wallimann, P.; Kennedy, R. J.; Miller, J. S.; Shalongo, W.; Kemp, D. S. *J. Am. Chem. Soc.* **2003**, *125*, 1203.
- (45) Sreerama, N.; Woody, R. W. In *Circular Dichroism: Principles and Applications*, 2nd ed.; Berova, N.; Nakanishi, K.; Woody, R. W., Eds.; Wiley: New York, 2000; pp 601–620.
- (46) Toniolo, C.; Crisma, M.; Formaggio, F.; Peggion, C. *Biopolymers* **2001**, *60*, 396 and references therein.